Approved For Release
2009/08/26 :
CIA-RDP88-00904R000100110

Third United Nations International Conference on the Peaceful Uses of Atomic Energy

A/CONF.28/P/375
USSR
May 1964
Original: ENGLISH

Confidential until official release during Conference

EXPERIMENTAL STUDY OF SOME METHODS OF COMPENSATING EXCESS REACTIVITY IN INTERMEDIATE REACTORS.

V.A.Kuznetsov, A.I.Mogilner, L.A.Chernov, V.V.Chekunov, V.I.Sharadin.

The work which is in part discussed in this paper aimed at analysing, in a comparative way, three possible methods of compensating excess reactivity in an intermediate reactor so as to determine their potentialities, advantages and drawbacks:

a) by means of a system of absorbing rods;

b) by means of control cylinders placed in the side reflector with their surface partially covered by a layer of absorber (See Refs. 1 and 2);

c) by separating two halves of the core in height.

No generality is chaimed for the absolute values of reactivity changes and distortion of the fields cited in the paper due to the obvious fact that such values are dependent on the size and composition of the core and reflectors as well as on the neutron spectrum in the reactor.

The experiments described below were carried out on the PF-4 assembly designed for studying the physical characteristics of intermediate reactors; the detailed description of this assembly is given in Ref. (1).

Reactivity changes were measured during the experiments by the reverse counting method and by method of increasing the core height.

The first method was used in subcritical experiments. It is based on a well-known equation which relates the changes in the

counting rate of an external detector (N_1-N_2) to the changes of reactivity (ΔK) in a subcritical system with a source:

$$\Delta K = C \frac{N_1 - N_2}{N_1 \cdot N_2} \qquad (1)$$

Coefficient C was found with the help of a reactivity standard - one of the regulating rods of the reactor. In the course of the experiments the value of C varied quite substantially due to the distortions of the neutron fields in the reactor. To eliminate the resultant error C was measured for each condition of the system.

Under the second method the negative reactivity given to a critical reactor was mainly compensated by addition to the core of fuel and moderator layers (in the same ratio as in the core) previously calibrated in the units of reactivity, and, to a lesser degree, by small displacement of the regulator.

The neutron flux distribution in the core was measured with the help of a small-size fission chamber having an outer diameter of 7 mm. The measurements were made at a power level of about 25 mW maintained by automatic regulator APPM (Ref.1), the ionization chamber of the regulator being used as a monitor. The small diameter of the fission chamber enabled it to be placed between the tubes so as to minimize the field distortion in measurements.

Experimental Investigation of Mutual Effect (Interference) of Absorbers [x].

A considerable amount of excess initial reactivity has often to be compensated by a large number of control rods-absorbers. Physical investigation of such reactors is hampered by the difficulties in determining the reactivity margin, due to mutual interference of the control rods as a result of which the full reactivity margin actually differs from the sum of control rod worths mesured separately in an initially critical reactor.

A special experimental study was undertaken on the PF-4 assembly to investigate the mutual effect (interference) of two absorbing control rods in uranium-beryllium assembly (PF-4-16)

x) The work was participated in by Y.G.Pashkin.

without reflector ($\rho_{Be} / \rho_{U^5} = 75$).

The cylindrical control rods 20 mm in diameter contained boron carbide with boron density of 1.7 gr/cm^3. One control rod (No.1) was placed near the centre of the core, while the other was capable of radial displacement. Measurements were carried out in subcritical experiments.

The interference term was measured using the following technique. First the worth ρ_{10} of one rod (rod No.1, for example) was measured in the absence of the other rod; then the worth ρ_{12} of the same (1st) rod was measured in the presence of the other rod. The interference term ρ_{12} describing the effect of the second rod on the worth of the first was found from the relation:

$$\rho_{12} = \rho_{10} + \Delta_{12} \qquad (2)$$

The worth of the second control rod in the presence of the first is equal to:

$$\rho_{21} = \rho_{20} + \Delta_{21} \qquad (3)$$

The total worth of two control rods ρ_{1+2} is equal to:

$$\rho_{1+2} = \begin{cases} \rho_{21} + \rho_{10} = \rho_{10} + \rho_{20} + \Delta_{21} \\ \rho_{12} + \rho_{20} = \rho_{10} + \rho_{20} + \Delta_{21} \end{cases} \qquad (4)$$

whence $\Delta_{21} = \Delta_{12}$

When studying the interference a relative unit of reactivity was used; this unit represented the worth of the assembly regulator per centimeter of the linear portion of its characteristics. The results of the measurements are summarized in Table 1.

The results of the experiments were analysed on a simple assumption that if Δ_{12} is relatively small ($\Delta_{12} \ll \rho_{10}; \rho_{12}$), its value is proportional both to ρ_{10} and to ρ_{20}, the proportionality factor depending on the distance x_{12} between the control rod axes:

$$\Delta_{12} = \rho_{10}\, \rho_{20}\, f(x_{12}) \qquad (5)$$

Fig.1 shows the experimental points which were calculated on the basis of the data given in Table 1 with the help of rela-

tion (5). The analysis of these data prompts the following conclusions:

a) the perturbation introduced by the central control rod extends to the entire reactor;

b) when distance between the control rods is small their total effectiveness is below the sum of unperturbed worths of these control rods;

c) beginning with a certain distance (in the given case it is 164 mm) the interference term changes its sign;

d) the dependence of the factor $f(x) = \Delta_{12} / \int_{10} \int_{20}$ on the distance is almost linear. Deviation of the proportionality factor f(x) from the linear dependence towards higher values of $\Delta(x)$ at short distances may be explained both by the fact that in this case the inequality $\Delta \ll \int$ is satisfied in the least degree and by the fact that the worth of the second control rod is additionally decreased by the shadow effect of the first rod.

T a b l e 1.

Distance between control rods (mm).	20	36	73	109	146	182
Efficiency of a single rod (linear cm).	216	213	191	148	110	77
Interferentional term Δ_{12} (linear cm).	-95	-67	-34	-21	- 8	3

The conclusion cited above refer to two control rods one of which is capable of radial displacement. However, the applicability of these conclusions is much wider. Fig.2 gives the data obtained on PF-4 assembly (with the same ratio $\int_{Be} / \int_{U^5}$, assembly PF-4-17) with the excess reactivity compensated by a group of control rods. In analysing the results of the experiments it was assumed that the combined effect of group of control rods on one of the rods can be treated as superposition of the effects of each rod in the group. In other words, it is assumed that if $\Delta \ll \int$ the interference is mainly accounted for by the twin interaction, i.e. the interaction of two control rods is not affected by the presence of other control rods.

375

Curve 1 in Fig. 2 shows $f(x_{ik}) = \Delta_{ik} / \rho_i \rho_k$, as a function of the distance between the control rod axes with the worths ρ_i and ρ_k measured in the presence of other control rods of the group. The linearity of $f(x_{ik})$ warrants the use of the superposition principle and can be employed for statistical alignment of the values of Δ_{ik} and sometimes for their prediction.

Assuming that the distance between the control rod axes is sufficiently great to cancel the "shadowing" and that the dependence of f(x) is linear a square symmetrical matrix with diagonal terms $\Delta_{ii} = \rho_{io}$ can be composed from the values of Δ_{ik} relating to two control rods (i,k); in this case ρ_{io} is the worth of the i-th control rod in the absence of all other control rods. The number of rows and columns of the matrix is equal to the number of the control rods. The part of the reactivity accounted for by some (i-th) control rod is equal to the sum of the matrix elements in the corresponding (i-th) column or row:

$$\rho_i = \Sigma_k \Delta_{ik} = \Sigma_k \Delta_{ki} \qquad (6)$$

When some control rod is removed the corresponding column and row must be stricken off. To obtain the effetiveness of the entire group of the control rods the diagonal terms and all terms above (or below) the diagonal must be summed up.

It can be easily seen that the measurement of $\Delta_{ik} (i \neq k)$ and ρ_i makes it possible to determine the value of ρ_{io} from the relation (6). Curve 2 in Fig. 2 shows the dependence $f_o(x) = \Delta_{ik} / \rho_{io} \rho_{ko}$. The two curves can be well approximated by straight lines intersecting the X-axis at the same point.

Investigation of Reactivity Control with the Help of Control Cylinders.

The experiments were carried out on the reactor PF-4-10 (Ref.3) with the core diameter of 417 mm and the ratio ρ_{Be} / ρ_{U^5} equal to 106. The equivalent thickness of the side beryllium reflector was 140 mm. The mockup of the control cylinder was designed as a hexagonal prism built up from 19 standard aluminium channels

375

(tubes) 50x1 mm dia. (Fig. 3). Six channels arranged in the outer row of the prism housed containers with boron carbide (γ_{B_4C} = 1.06 gr/cm^3) which simulated the absorbing layer of the control cylinders. The height of the absorbing layer was equal to the height of the core. The remaining 13 channels were the conventional channels of the beryllium reflector. The construction of the mockup provided for changing the thickness of the absorbing layer (5 and 10 mm), varying the curvature of the absorber, forming an air gap between the core and the control cylinder and turning the control cylinders discretely in steps of 30°. Turning of the control cylinders was simulated by the successive rearrangement of the channels with the absorber.

Fig. 4 schematically shows the control cylinders in various positions. To find the effectiveness of the control cylinder with a so-called "neutron trap" three conventional channels filled with paraffine to the height of the core were installed in the control cylinder behind the absorbing layer. All experiments were carried out with single control cylinders.

a) Effectiveness of Control Cylinder Versus Turn Angles.

Table II and Fig. 5 summarize the measurements of the control cylinder effectiveness as a function of the turn angle, which were carriedout atthe assembly PF-4-10 for a single control cylinder with the absorber curvature θ = 180° and absorber thickness δ_{B_4C} = 5 mm. The effectiveness of the control cylinder $\frac{\Delta K}{K}\Big|_{15°}^{\varphi}$ was found as the change in the system reactivity caused by turning the control cylinder from the position of the minimum system reactivity at φ = 15° (when the absorbing surface of the control cylinder is at a minimum distance to the core) to position φ .

These experiments were also used to determine the effect of the air gap between the core and the control cylinder on the cylinder effectiveness. For this purpose containers with boron carbide were removed from the mockups and reactivity changes were measu-

375

T a b l e II.

Control cylinder rod position (deg.) φ	Compensation capacity of cylinder $\frac{\Delta K}{K}$ [%] Method of inverse count	Method of add loading of fuel	The same without reactivity by air gap
15° (375°)	0.00	0.00	0.00
30° (0°, 360°)[x]	0.06	0.06	0.06
60° (330°)	0.785	0.79	0.575
90° (300°)	1.685	1.85	1.255
120° (270°)	2.51	2.74	1.764
150° (240°)	3.17	3.28	2.31
180° (210°)[x]	3.84	3.77	2.91
195°	3.90	3.85	2.97

[x] The reactivity change is obtained with the interpolate curve when cylindrical rod positions vary from 30° to 15° and from 180° to 195°.

red with the control cylinder turned from position φ =30° to position φ = 180° in steps of 30°. These measurements made it possible to determine the characteristics $\frac{\Delta K}{K} = f(\varphi)$ of the control cylinder with and without consideration of air gap. The "spurious" reactivity from the control cylinder was found by the change in the critical position of the regulator with the control cylinder mockup inserted into the reflector of an unperturbed reactor in the position of the maximum system criticality (φ = 210°); the spurious reactivity $\frac{\Delta K}{K}$ equalled 0.32%.

The data given in Table II and Fig. 5 indicate a substantial agreement between the measurements of the control cylinder effectiveness made in various positions of the cylinder by the accepted methods. The discrepancies in the measurement results are within the accuracy tolerances of the experiments.

b) Effectiveness of Control Cylinder Versus Absorber Curvature.

The qualitative analysis of the changes of the effectiveness

of the control cylinder depending on the curvature of the cylinder absorbing surface points out to the existence of an optimum curvature which provides the maximum effectiveness of the control cylinder at minimum "spurious" reactivity. To find the optimum curvature of the absorber experiments were staged on assembly PF-4-10 to find the reactivity changes brought about by the control cylinder in the positions of the minimum and maximum system reactivity for the cylinder mockups with the absorber curvature $\theta = 180^{\circ}$, 150° and 120° at $\delta_{a.c} = 5$mm. The absorber curvature was varied by substituting the channels containing the absorber with the usual channels of the beryllium reflector.

The results of the measurements made on the assembly PF-4-10 are given in Table III. The tabular data show that out of the three curvatures the optimum curvature of the control cylinder absorber for the reactor PF-4-10 is approximately 120°; the cylinder with this curvature has the maximum effectiveness and minimum "spurious" reactivity. Analysing the reactivity change brought about by the control cylinder in the position $\varphi = 0$ it can be expected that further reduction of the absorber curvature will result in the decreased effectiveness of the cylinder.

c) Effectiveness of Control Cylinder Versus Absorber Layer Thickness

The variation of the effectiveness of the control cylinders as a function of the absorber layer thickness was studied on the assembly PF-4-10. The measurement results indicate that the effectiveness of a control cylinder with the absorber curvature $\theta = 150^{\circ}$ increases 1.27 times as the thickness of the boron carbide layer is increased from 5 to 10 mm.

d) Effectiveness of Control Cylinder with "Neutron Traps".

The experiment was carried out on the assembly PF-4-10 with a control cylinder mockup having the following characteristics: $\theta = 180^{\circ}$, $\delta_{a.c} = 5$ mm. It has been established that three paraffin-filled channels placed in the control cylinder behind the

375

layer of boron carbide increased the effectiveness of the control cylinder by $\frac{\Delta K}{K} \simeq 1\%$. This was attended by an increase in the negative "spurious" reactivity equalling $\frac{\Delta K}{K} \simeq 0,12\%$.

e) Fission Density Distributions Along the Core Radius in Various Positions of the Control Cylinder.

It can be assumed that the control cylinder does not produce any appreciable distortion of the distribution along the height of the core. Therefore the experiments were confined to studying the distortions of the neutron field along the core radius and along the core boundary in the area where the control cylinder was located. The distributions were measured both for an unperturbed system and for perturbations introduced by a single control cylinder in the positions $\varphi = 270^\circ$ and $\varphi = 30^\circ$. The position of the chamber in height corresponded to the centre of the core.

The results of the distribution measurements in the direction "core centre-control cylinder centre" (AA' in Fig.3) are shown in Fig.6. Since the distribution measurements in various positions of the control cylinder were made at different power levels the fission density distributions were referred to the value in the core centre.

Fig.7 shows the fission density distributions along the perimeter of the core in the area where the control cylinder is located; these distributions are referred to the value of the fission density in the core center unperturbed by the action of the control cylinder.

Investigation of Reactivity Control by Core Separation.

The method where by the reactivity was controlled by moving apart the two halves of the core was investigated on assemblies PF-4-09, PF-4-13, PF-4-10 and PF-4-12 (with the nuclear concentrations ρ_{Be} / ρ_{U^5} varying within the range from 0 to 106).

The reactivity changes brought about by the core separation with the resultant increase in the neutron leakage were measured in the subcritical condition by the reverse counting method

with one of the regulating rods used as a reactivity standard. It was assumed that the worth of the rod was not affected markedly by the core separation, which was experimentally shown to be true for separations up to 40 mm.

Fig.8 shows how the core was moved apart. This was accomplished with the help of thin-walled aluminium tubes inserted between the halves of the core. All experiments were confined to separation of the core only. On two assemblies the reactivity changes due to the core separation were compared against the reactivity changes brought about by uniform "dilution" of the cores with respect to uranium and beryllium at the same core diameter and with the corresponding increase in the height of the core.

Table III shows the reactivity changes caused by the core separation in various assemblies. The corresponding data for the assemblies PF-4-09 and PF-4-10 are given in Fig.9.

As can be seen from Table III and Fig.9 the effectiveness of core separation by 1cm increases with decreasing $\rho_{BE}/\rho_{U^{5}}$ which is mainly due to the reduction in the assembly size at smaller $\rho_{Be} / \rho_{U^{5}}$.

T a b l e III.

Assembly	Value of splitting ΔH (mm)	Efficiency by splitting into two equal halves $\frac{\Delta K}{K}$ [%]		Efficiency of uniform "delution" equivalent to splitting into value	ΔH, $\frac{\Delta}{K}$ [%]
	10	1.76	0.07		-
PF-4-09	20	3.20	0.16	3.17	0.14
	30	5.14	0.35		-
	40	6.96	0.53		-
	10	0.85	0.05		-
PF-4-13	20	1.90	0.05		-
	40	3.20	0.05		-
	80	4.0	0.06		-
	10	0.78	0.004		-
	20	1.365	0.017		-
	40	2.56	0.18		-
PF-4-10	80	4.77	0.18		-
	160	0.50	0.75		-
PF-4-12	40	3.71	0.21	2.68	0.20

The effectiveness of core separation into two halves was compared against the effectiveness of uniform core expansion by means of air dilution. Such comparison has shown that the values of the effectiveness are related to each other as the squares of the fast neutron flux in the centre of the core and the average value of the flux along the height. This can be understood considering the fact that the portion of the reactivity accounted for by fast neutrons escaping through the gap (these neutrons primarily determine the effectiveness of core separation) is proportional to the product of their flux by importance.

Apart from the reactivity changes, a problem that also merits attentions is the fission density distribution along the height of a core with a horizontal central gap.

The distribution of fission density along the core height was measured with the help of a fission chamber with 30mm. separations for the assembly PF-4-09 and 40 mm separation for the assembly PF-4-10. The measurement results are shown in Figs. 10 and 11. The charts given in these figures indicate that in the core areas bordering on the gap and on the side reflector the fission density rises due to the inflow of moderated neutrons from the side reflector.

REFERENCES.

1. A.I.Leipunskii V.A.Kuznetsov, G.Y.Artukhov, A.I.Mogilner, Y.A.Prokhorov, V.M.Steklovskii L.A.Chernov.
   Experimental Study of Some Physical Characteristics of Intermediate Reactors with Beryllium Moderator.
   Paper SM 18/80 presented to the Vienna Seminar on the Physics of Fast and Intermediate Reactors, 1961.

2. The Physics of Intermediate Spectrum Reactors, Editor I.R. Stehn, US AEC, 1958.

3. I.I.Zakharkin, V.A.Kuznetsov, I.E.Somov, L.A.Chernov et al. Neutron-Physical Investigations of U-Be and U-BeO Systems. Paper presented to the 3rd Geneva Conference on the Peaceful Use of Atomic Energy.

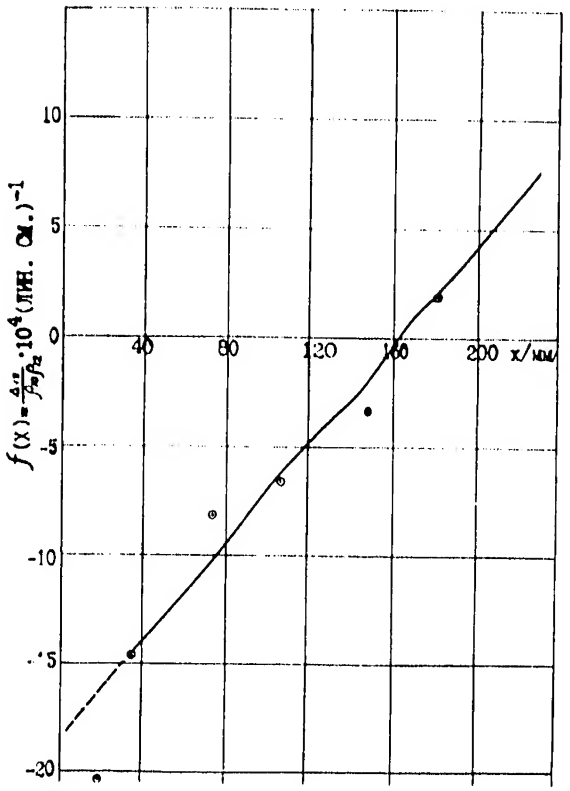

Fig. 1. $f(x) = \frac{\Delta_{12}}{\rho_{10}\,\rho_{20}}$ as a function of the distance between the control cylinder axes.

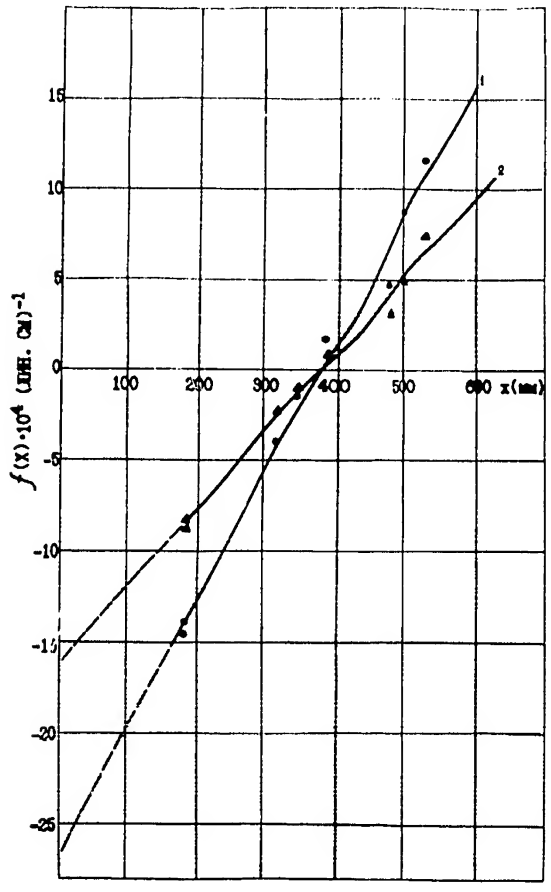

Fig. 2. $f(x)_k = \frac{\Delta_{ik}}{\rho_i\,\rho_k}$ (curve 1) and $f_{(x_i)} = \frac{\Delta_{ik}}{\rho_{io}\,\rho_{ko}}$ (curve 2) as functions of the distance between the control cylinder axes.

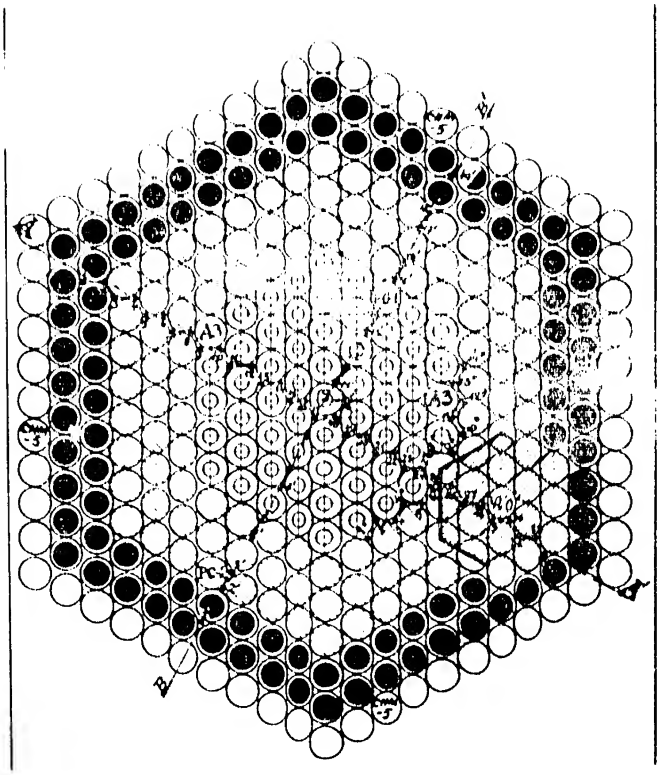

Fig. 3. Sketch of the critical assembly PF-4-10 with a control cylinder in the position $\varphi = 0^0$.

- source
- steel reflector
- core stack
- tor stack
- beryllium reflector stack
- control rod
- safety rod
- BF_3-counter
- 1,2,3,... , n- Nos. of the points at which the neutron field was measured.

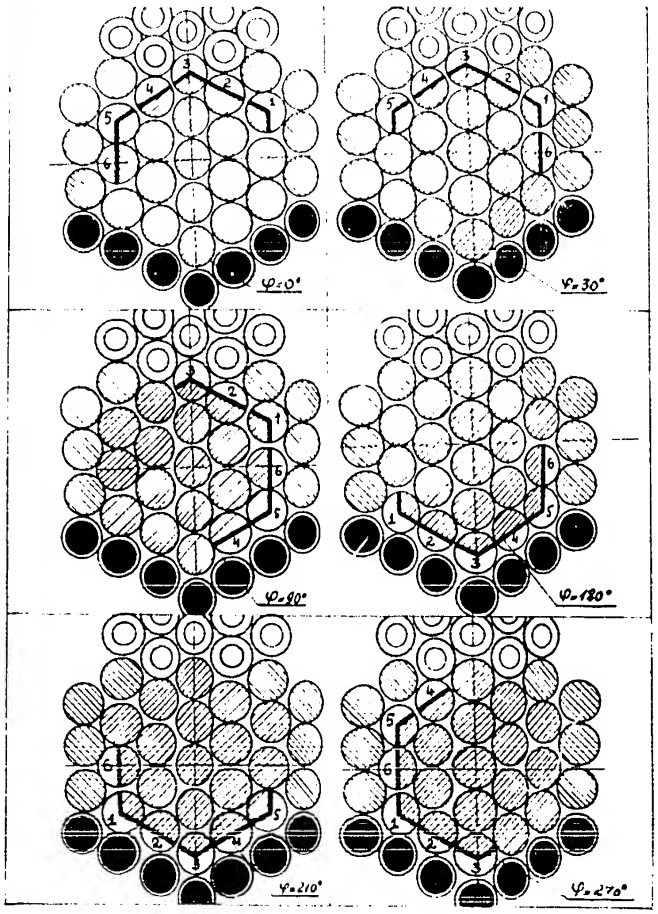

Fig. 4. Various positions of a single control cylinder in the critical assembly PF-4-10

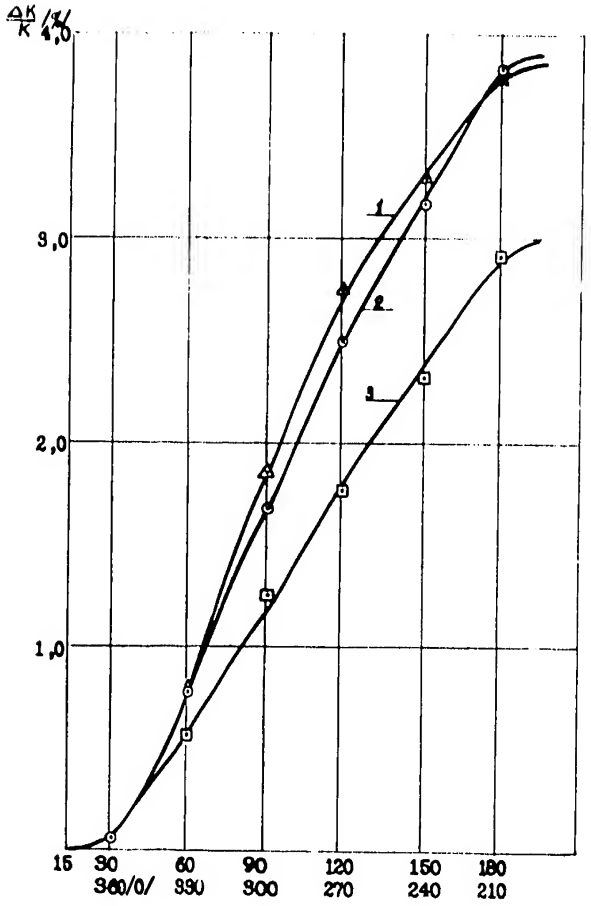

Fig 5. Characteristics of a control cylinder.
1- method of additional loading of core material,
2- reverse counting method,
3- characteristic of the control cylinder minus the effect of the air gap.

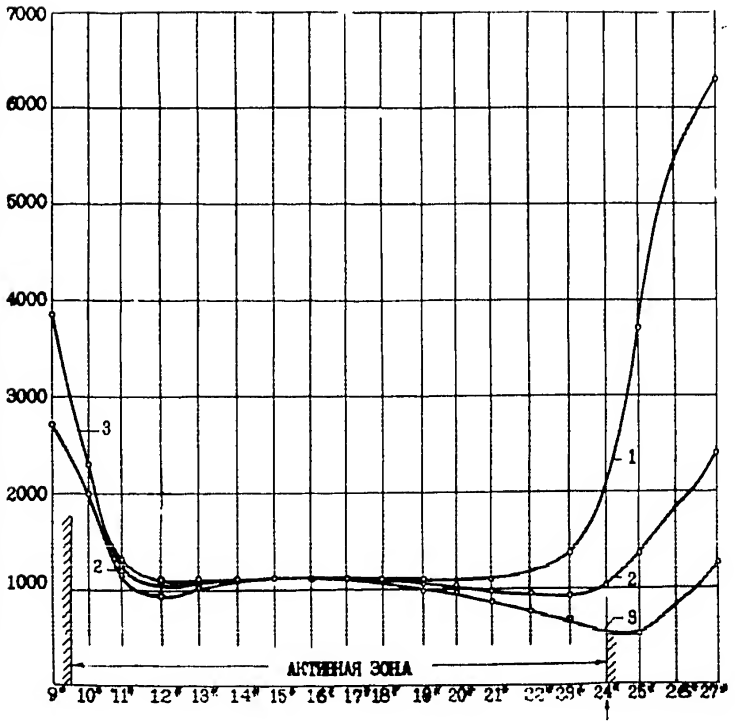

Fig. 6. Fission density distribution measured with uranium fision chamber along the radius of the reactor PF-4-10 in the direction AA' (Fig.3) (referred to the value in the core centre).
1 - unperturbed distribution,
2 - the distribution for the control cylinder in position $\varphi = 270^{\circ}$,
3 -distribution for the control cylinder in pisition $\varphi = 30^{\circ}$.

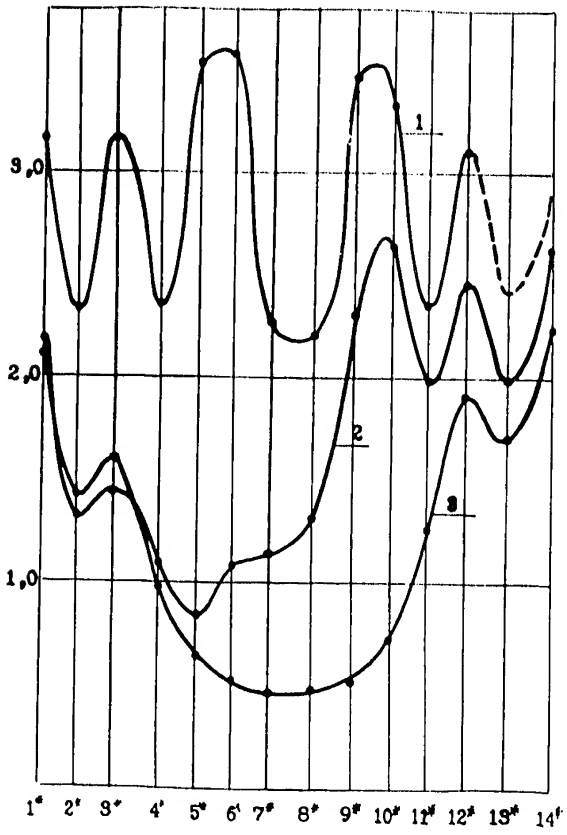

Fig. 7. Fission density distribution measured with uranium fission chamber along the core perimeter of the reactor PF-4-10 in the area where the control cylinder is located. All curves are referred to the fission density in the core centre unperturbed by the action of the control cylinder.

1-unperturbed distribution,
2-distributions for the control cylinder in position $\varphi = 270^{\circ}$;
3-distributions for the control cylinder in position $\varphi = 30^{\circ}$.

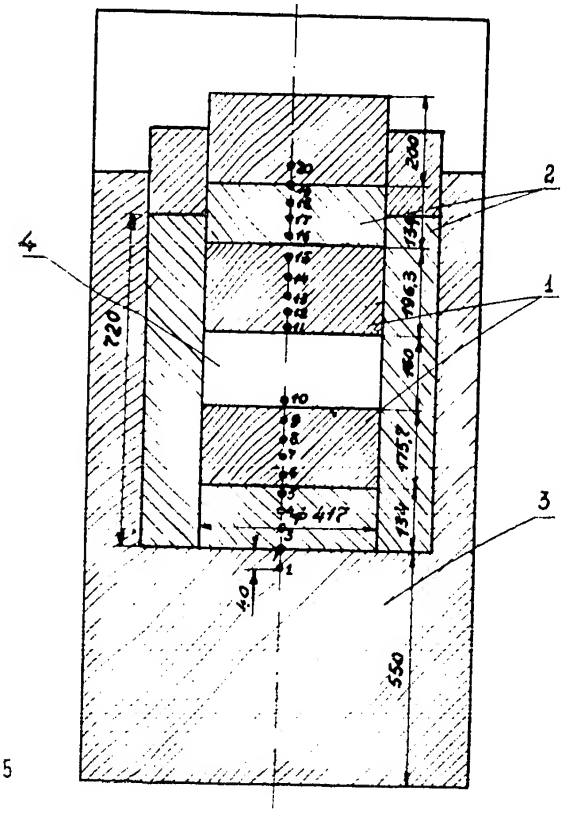

Fig. 8. Core separation in the reactor PF-4-10.

1 - core,
2 - beryllium reflector,
3 - steel reflector,
4 - intermediate air layer.

375

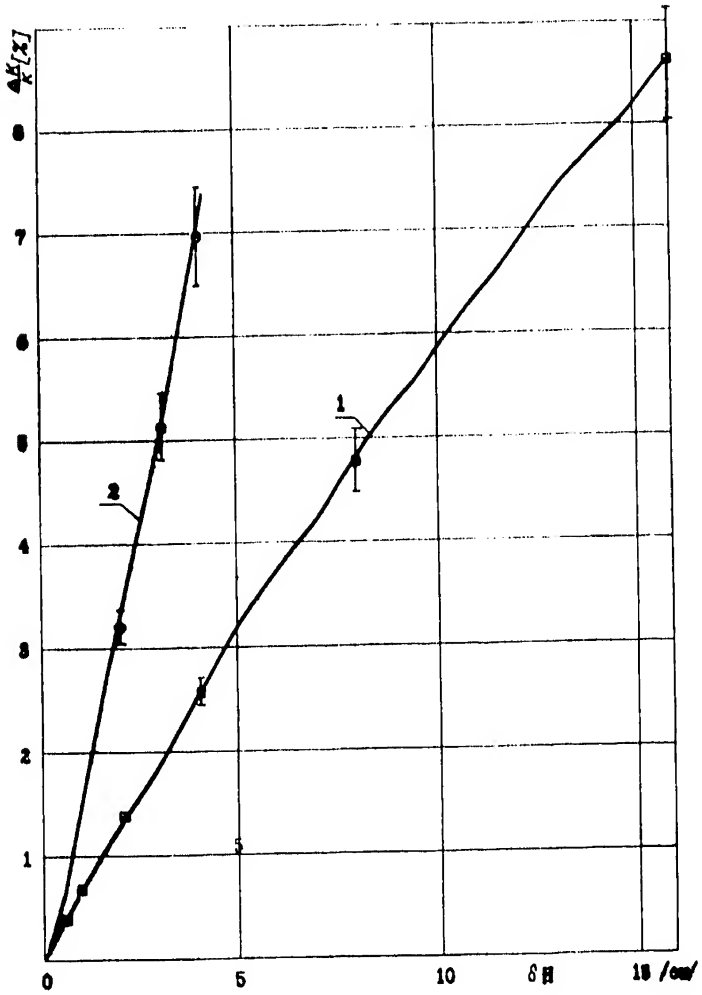

Fig. 9. Variation of the system reactivity caused by separation of the reactors in the PF-4 assembly.

1 - assembly PF-4-13,

2 - assembly PF-4-10.

375

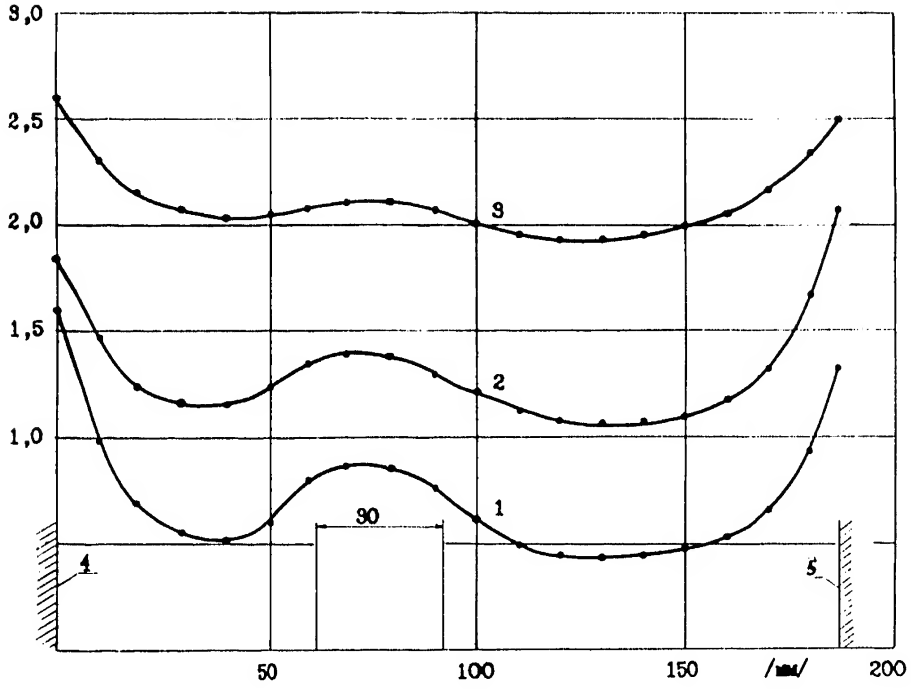

Fig. 10. Fission density distribution along the core height in the critical assembly PF-4-09 at $\rho_{Be} / \rho_{US} = 0$ at various radial points, measured with uranium fission chamber. The distributions are referred to the value in the core centre at zero separation.

1- r = 29.5 mm (in the core),
2- r = 59.0 mm (at the boundary with the reflector),
3- r =118 mm (in the reflector).

375

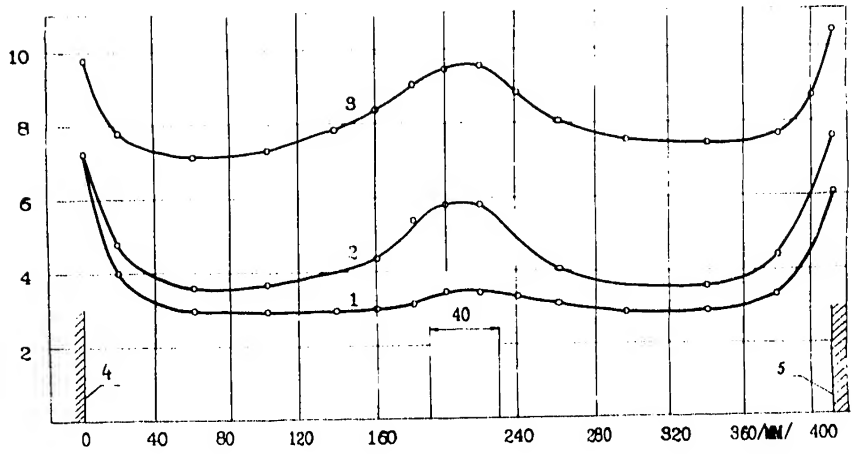

Fig. 11. Fission density distribution along the core height in the critical assembly PF-4-10 at ρ_{Be} / ρ_{U5} = 106 at various radial points, measured with uranium fission chamber. The fields are referred to the value in the core centre at zero separation.

1- r = 29.5 mm (point 16 in Fig.3),
2- r =147.0 mm (point 6 in Fig.3),
3- r= 206 mm (point 3 in Fig.3).

375

CAPTIONS TO FIGURES.

Fig. 1. $f(x) = \frac{\Delta_{12}}{\rho_{1\infty}\,\rho_{2\infty}}$ as a function of the distance between the control cylinder axes.

Fig. 2. $f(xi)_k = \frac{\Delta_{ik}}{\rho_i\,\rho_k}$ (curve 1) and $f_{(x)} = \frac{\Delta_{ik}}{\rho_{i\infty}\,\rho_{k\infty}}$ (curve 2) as functions of the distance between the control cylinder axes.

Fig. 3. Sketch of the critical assembly PF-4-10 with a control cylinder in the position $\varphi = 0^\circ$.

- source
- core stack
- beryllium reflector stack
- steel reflector stack
- PC - control rod
- A3 - safety rod
- ENMS - BF_3-counter
- (i) 1,2,3, . . . ,n - Nos. of the points at which the neutron field was measured.

Fig. 4. Various positions of a single control cylinder in the critical assenbly PF-4-10.

Fig. 5. Characteristics of a control cylinder.
1 - method of additional loading of core material,
2 - reverse counting method,
3 - characteristic of the control cylinder minus the effect of the air gap.

Fig. 6. Fission density distribution measured with uranium fission chamber along the radius of the reactor PF-4-10 in the direction AA' (Fig.3)(referred to the value in the core centre).
1 - unperturbed distribution,
2 - the distribution for the control cylinder in position $\varphi = 270^\circ$,
3 - distribution for the control cylinder in position $\varphi = 30^\circ$.

Fig. 7. Fission density distribution measured with uranium fis-

sion chamber along the core perimeter of the reactor PF-4-10 in the area where the control cylinder is located. All curves are referred to the fission density in the core centre unperturbed by the action of the control cylinder.

1 - unperturbed distribution,

2 - distributions for the control cylinder in position $\varphi = 270^{\circ}$;

3 - distributions for the control cylinder in position $\varphi = 30^{\circ}$.

Fig. 8 .Core separation in the reactor PF-4-10.

1 - core,

2 - beryllium reflector,

3 - steel reflector,

4 - intermediate air layer.

Fig. 9. Variation of the system reactivity caused by separation of the reactors in the PF-4 assembly.

1 - assembly PF-4-13,

2 - assembly PF-4-10.

Fig.10. Fission density distribution along the core height in the critical assembly PF-4-09 at $\rho_{Be} / \rho_{U5} = 0$ at various radial points, measured with uranium fission chamber. The distributions are referred to the value in the core centre at zero separation.

1 - r = 29.5 mm (in the core),

2 - r = 59.0 mm (at the boundary with the reflector),

3 - r = 118 mm (in the reflector).

Fig.11. Fission density distribution along the core height in the critical assembly PF-4-10 at $\rho_{Be} / \rho_{U5} = 106$ at various radial points, measured with uranium fission chamber. The fields are referred to the value in the core centre at zero separation.

1 - r = 29.5 mm (point 16 in Fig.3),

2 - r = 147.0 mm (point 6 in Fig.3),

3 - r = 206 mm (point 3 in Fig.3).

375